Upper-Level Features Associated with Winter Monsoon Surges over South China

M. C. WU AND JOHNNY C. L. CHAN

Department of Physics and Materials Science, City University of Hong Kong, Kowloon, Hong Kong

(Manuscript received 25 August 1995, in final form 8 April 1996)

ABSTRACT

The upper-level features associated with the two kinds of winter monsoon surges over south China are studied: the easterly surge (ES) and the northerly surge (NS). The study is similar to that used by Wu and Chan, except that a broader region (0°–60°N, 70°–160°E) is considered.

The outbreak of an NS is associated with a breakdown of the Siberia–Mongolia high. The upper-level features suggest that the evolution of the Siberia–Mongolia high in an NS can be related to an eastward passage of a short-wave trough and the polar jet based on the quasigeostrophic theory. The intensification of the Siberia–Mongolia high appears likely to be caused mainly by the adiabatic cooling due to rising motion associated with the trough and the polar jet passages. After the passage of the trough and the jet, the Siberia–Mongolia high breaks down in response to the sinking motion upstream of the trough, causing a surge of the northerly winds over the south China coast.

For the ES, the passage of an upper ridge is observed. The zonal index increases in an ES but the subtropical jet weakens. The high pressure center responsible for the ES (the Dahingganling high) is found to be a split cell from the Siberia–Mongolia high, and the splitting is related to the ridge passage. A temperature inversion is only observed when the high is not far from the parent high (i.e., Siberia–Mongolia high). Unlike the NS, an ES is found not to be associated with a strong north–south thermal contrast. Significant differences are observed when comparing the features of the ES and NS. On the whole, the results from this study and those from Wu and Chan suggest that on the synoptic scale a clear distinction exists between the ES and NS on the synoptic scale both at upper levels and the surface.

1. Introduction

The surface features associated with the two types of winter monsoon surges over south China, namely the easterly surge (ES) and the northerly surge (NS), have been documented by Wu and Chan (1995). An ES is basically defined as a strong easterly wind event, while an NS is defined as an abrupt daily mean temperature drop of greater than 2°C with surface winds turning to the north over Hong Kong. In the definition of the surges, day 0 is labeled as the day the surge arrived in Hong Kong.

At the surface, an ES occurs due to the eastward movement of a surface high pressure center from Dahingganling (45°N, 100°E). When the high migrates to the Yellow Sea, coastal ridging along the southeast China coast is observed, consistent with the strongest easterly winds over Hong Kong on day 0. While temperature variations are not significant over mainland China, stations along the southeast China coast can have a temperature rise of approximately 1°–2°C after the ES with an increase in relative humidity.

On the other hand, an NS occurs with the breakdown of the Siberia–Mongolia high and is associated with a cold front passage. The Siberia–Mongolia high intensifies to above 1045 hPa [the mean sea level pressure (MSLP)] before it collapses and an NS is initiated. Cold air pushes southward swiftly and soon reaches the South China Sea within 2 days, causing surface temperature drops of approximately 4°–5°C in most parts of China. It is evident that the relative humidity decreases when the NS arrives. On the whole, the two types of surges have clear distinctive surface characteristics.

The present paper represents the second part of the paper by Wu and Chan (1995) with the same surges considered and the same methodology used. It presents the synoptic-scale features in the lower and upper troposphere for the ES and NS. A major objective is to find out and compare the synoptic-scale upper-level features associated with the surges. In the present study the region is extended to 0°–60°N, 70°–160°E (see Fig. 1). The time span representing the surge episode is from day −3 to day 3 but parameters between day −7 and day 7 will be considered to show the temporal variations. Global Telecommunication System data are used with the average of the 0000 and 1200 UTC data denoting the daily value. All data

Corresponding author address: Dr. Johnny C. Chan, Dept. of Physics and Materials Science, City University of Hong Kong, Tat Chee Avenue, Kowloon, Hong Kong.
E-mail: apjcchan@cityu.edu.hk

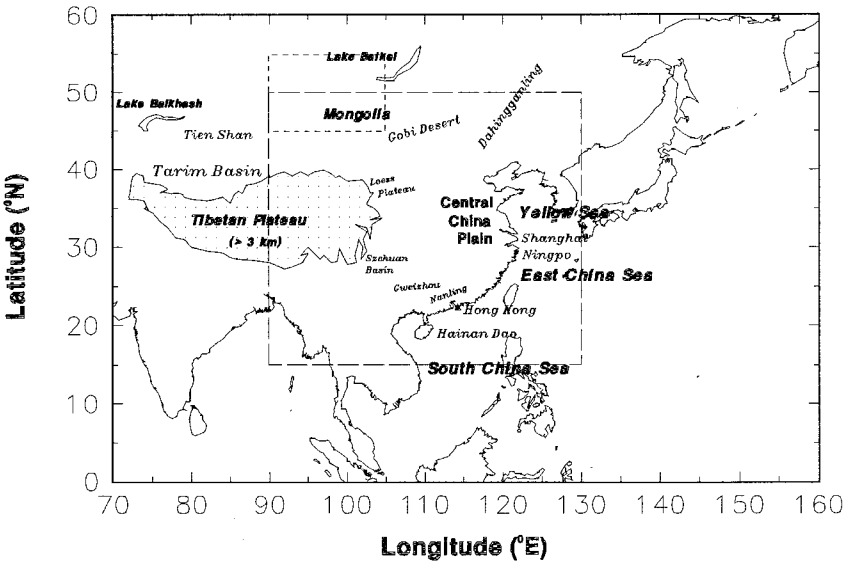

FIG. 1. The region covered in the synoptic-scale study and some geographic names. The long- and short-dashed lines define the area considered at the surface and the Siberia–Mongolia region, respectively. The shaded region shows the Tibetan Plateau with altitude greater than 3 km.

are interpolated into 2.5° × 2.5° latitude–longitude gridded values when needed (see Wu and Chan 1995 for details). Calculation of various dynamic parameters such as the vorticity and advection are all based on these gridded values.

The upper-level features associated with the NS and ES will be considered in sections 2 and 3, respectively. Analyses involve temporal variations of the zonal index, evolution of the Siberia–Mongolia high, the quasigeostrophic forcing (QG), and the passage of upper waves, etc. Comparisons between the two types of surges are considered in the study of the ES. Section 4 gives a summary of the study from which coherent physical models for the surges are developed.

2. Northerly surge

a. Lower-tropospheric features

The geopotential height at 1000 hPa on day 0 (Fig. 2) shows clearly the Siberia–Mongolia high, which is

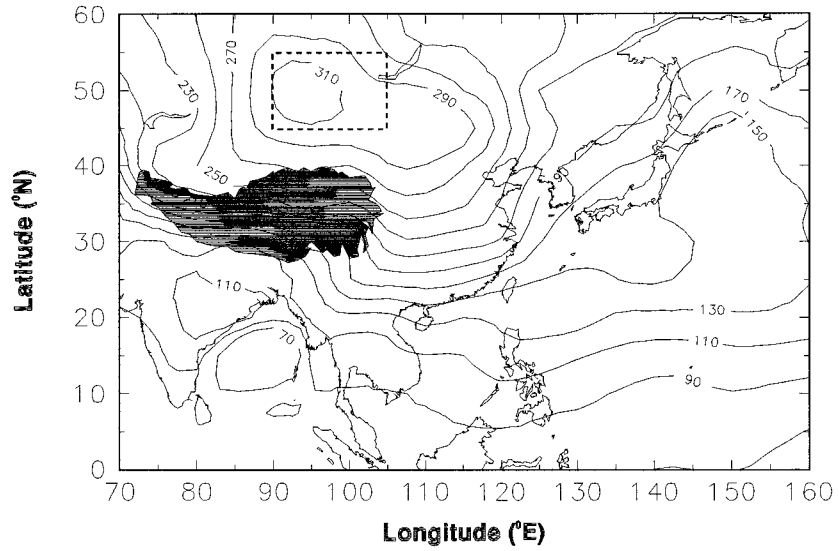

FIG. 2. The 1000-hPa geopotential height (m) of an NS on day 0. The dashed lines define the region of Siberia–Mongolia. Blackened area indicates the Tibetan Plateau with altitude greater than 3 km.

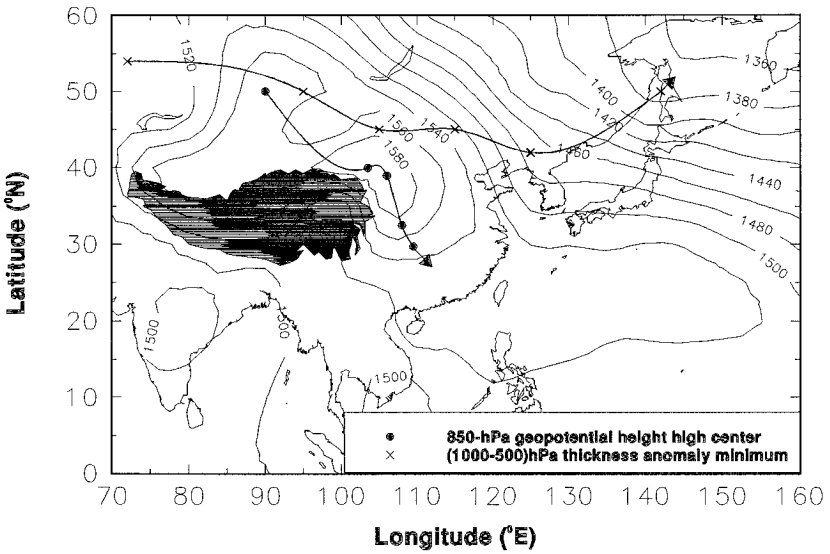

FIG. 3. The 850-hPa geopotential height of an NS on day 0. The solid curves show the track of the high height center from 1200 UTC day −1 to 1200 UTC day 1 (bottom track, dots every 12 h) and the 1000–500-hPa thickness anomaly minimum from day −3 to day 2 (top track, crosses every 12 h).

consistent with that observed over the surface (see Wu and Chan 1995). The region where the high is located (i.e., 45°–55°N, 90°–105°E) will be designated as the domain for studying the evolution of the Siberia–Mongolia high later. The high is well defined after day −2, and no significant motion of it can be observed during the NS, but the height increases from about 280 to 310 m after day −1 and decreases after day 2 (not shown). On the other hand, the Siberia–Mongolia high at the 850-hPa level is smaller in horizontal scale and is not very clear until day −1, which suggests that the shallow high has intensified significantly and just penetrated into the 850-hPa level by that time. Figure 3 shows the pattern on day 0. Furthermore, the 850-hPa high moves from 1200 UTC day −1 to 1200 UTC day 2 in a northwest–southeast track (see Fig. 3), which is very similar to that of the 1000-hPa high center in the composite study of 19 cold outbreaks events by Ding and Krishnamurti (1987). The locations of the minimum thickness anomaly in the 1000–500-hPa layer from day −3 to day 2 shown in Fig. 3 suggest that the lower-tropospheric cold air mass is migrating eastward, and it will be clear later that the migration is consistent with a trough passage at 500 hPa. Further, the locations of the 850-hPa high between 1200 UTC on day −1 and 1200 UTC on day 0 lag behind the center of the cold air mass (as represented by the minimum thickness anomaly) such that the transient development of the 850-hPa high center may be attributed to the sinking of the cold air. If the minimum 1000–500-hPa thickness anomaly is taken to represent the approximate mean position of a trough aloft, the track of the 850-hPa high would therefore be consistent with the air parcel trajectory projecting on the 850-hPa surface behind a cold front in a developing baroclinic wave (e.g., Holton 1979, his Fig. 6.12). Thus, the 850-hPa high probably represents a cell of cold air moving along a southward trajectory.

b. Midtropospheric trough and short wave

The eastward passage of a northeast–southwest-oriented trough is observed from the 700-hPa geopotential charts (not shown). As the trough–ridge evolution in the geopotential height patterns is not very evident, variation in the trough propagation is investigated indirectly by referring to the zonal index and Hovmöller diagram.

1) ZONAL INDEX

A preliminary view of the upper-level flow pattern can be obtained by studying the variation of the 500-hPa westerly zonal index (I_z) computed over the region 40°–50°N, 70°–130°E in Fig. 4. The index is defined as

$$I_z = \frac{\sum (H_1 - H_2)}{\phi_2 - \phi_1},$$

where H is the 500-hPa height; ϕ is the latitude; the subscripts 1 and 2 represent values at 50° and 40°N, respectively; and the summation is taken from 70° to 130°E at 2.5° longitude intervals. Consistent with Bao (1987), the NS or cold outbreak occurs when the index

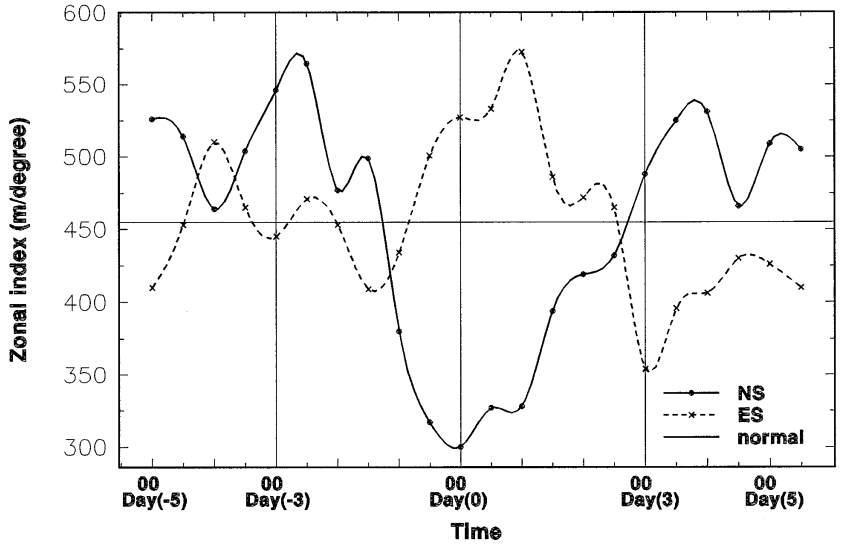

FIG. 4. The westerly zonal index of an ES, an NS, and as normal. Time reference lines are shown at 0000 UTC on day −3, day 0, and day 3.

changes from high to low value. The lowest index occurs on day 0, which is consistent with the large-scale northerly surge (surface meridional flow) sweeping across China (see Wu and Chan 1995). The contrast in the circulation patterns between the NS and either the normal condition or the ES is particularly evident. Following the end of the NS and the perturbation of the meridional flow, the circulation gradually resumed being zonal. Based on the variation of the index, the whole process (i.e., the change over between zonal and meridional circulations) associated with the NS takes around 6 days, which is longer than the time span associated with the surface features. Clearly, the NS indeed represents a kind of large-scale flow adjustment in the atmosphere.

2) HOVMÖLLER DIAGRAM

The change in circulation pattern can be understood by referring to the Hovmöller diagram showing the 500-hPa height anomaly averaged between 30° and 50°N (Fig. 5a). It can be seen that a trough is initially located at around 90°–100°E (or farther west) on around day −2, propagates eastward, and then deepens mostly by day 1 and day 2 in the vicinity of 130°E and becomes a deep longwave trough. The propagation of the trough is estimated to be approximately 13 m s^{-1} (25° longitude per 2.5 days), which agrees with that of a typical shortwave. In fact, the rapid change in the zonal index shown in Fig. 4 implies a fast-moving shortwave passage during an NS. This is consistent with a forecasting criterion of the Royal Observatory of Hong Kong (ROHK) (Chu 1978) that an NS (cold surge) will reach Hong Kong within 2 days of the passage of a 500-hPa trough over Lake Baikal (100°–110°E). Also shown is the 700-hPa trough, which leads ahead of the 500-hPa trough by around 1 day. [An anlysis of the 700-hPa geopotential height (not shown) suggests a trough oriented northeast–southwest that propagates eastward from day −1 to day 0 and deepens by day 0.]

The long-wave trough is the deepest by day 1 after the occurrence of the NS, so it is likely that the outbreak of the surge is not directly related to the deepening of the longwave trough but rather the reverse. The NS occurs and the lowest zonal index is reached just when the short wave merges with the long wave on day 0. On the whole, the development and propagation of a short wave is one of the basic ingredients of the NS.

Furthermore, a time lag is observed (Fig. 5b) between the 700–500-hPa thickness trough and the 500-hPa height trough indicating the cold advection upstream of the short wave. This time lag between the thermal and height troughs and the westward tilt of height trough are consistent with a developing baroclinic wave (e.g., Holton 1979).

c. Jet stream

The zonal winds at 500 hPa from day −3 to day 1 show that the subtropical jet stream is in the vicinity of the southern flank of the Tibetan Plateau with the jet core over south of Japan (Figs. 6a–e). From day −3 to day −1, the zonal winds over the northern vicinity of the Tarim Basin (i.e., the northern flank of the Tibetan Plateau) are strengthening and propagate eastward. This strengthening in the westerlies can be regarded as the passage of the polar jet (or the northern

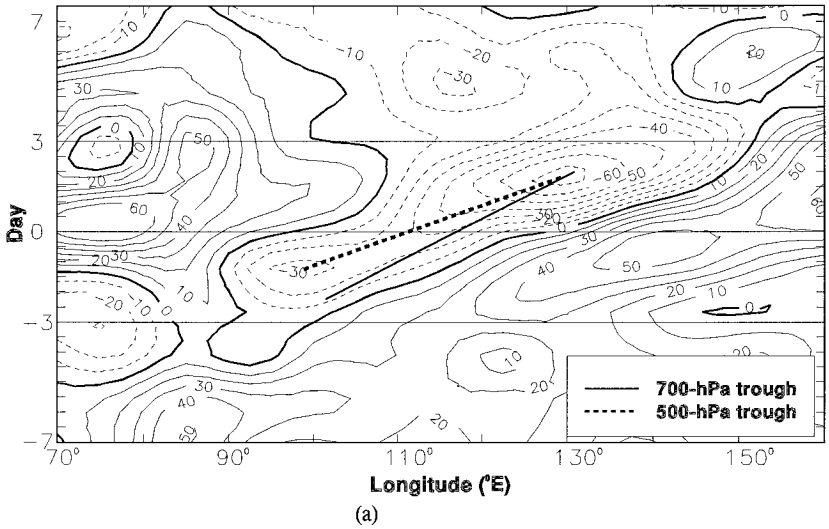

FIG. 5. Time–longitude cross section of (a) 500-hPa geopotential height anomaly (with the 700-hPa trough superimposed) and (b) 700–500-hPa thickness anomaly (with the 500-hPa trough superimposed) of an NS. All data are averaged between 30° and 50°N.

jet) from the west of Lake Balkhash (45°N, 75°E). The polar jet is migrating eastward during this time, which in fact corresponds to the propagation of the short wave (trough) discussed above. By day −1, the subtropical jet merges together with the polar jet at about 120°E. (It should be pointed out that the polar jet is less pronounced than the subtropical counterpart in strength during the wintertime so that only the latter is evident in the composite chart.) After day −1, the subtropical jet strengthens with maximum strength attained on and after day 1.

The passage of the polar jet can be seen more clearly by studying the zonal wind anomaly. Figure 6f shows the zonal wind anomaly on day −2 with the approximate positions of the maximum anomaly from day −5 to day −1. It can be seen that a center of positive zonal wind anomaly, which is located at around 45°N, propagates from the west of Lake Balkhash on day −5 to the south of Lake Baikal (southern boundary of the Siberia–Mongolia region) by day −2 after passing over the Tarim Basin. The belt of positive zonal wind anomaly (analogous to a jet streak), which lies over the northern flank of the Tibetan Plateau on day −1, turns to the southern flank of the Tibetan Plateau from day 0 onward with the magnitude of the anomaly maximum increasing and shifting southeastward.

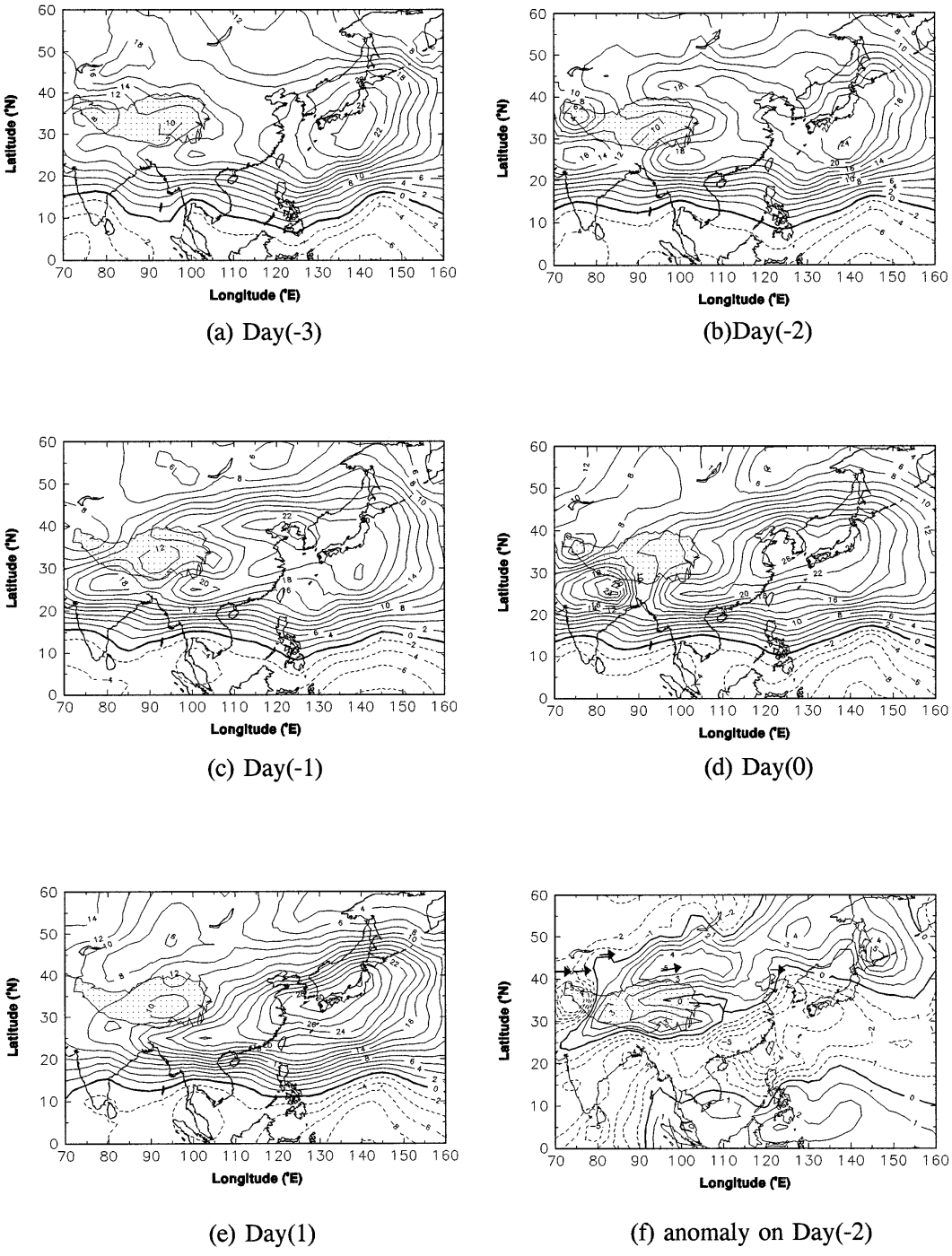

FIG. 6. (a)–(e) The 500-hPa zonal wind of an NS from day −3 to day 1 and (f) the 500-hPa zonal wind anomaly on day −2. The arrows in (f) show the position of the anomaly maximum from day −5 (leftmost arrow) to day −1 (rightmost arrow). Stippled region indicates the Tibetan Plateau.

When the subtropical jet and the polar jet merge on around day −1 and become a major jet stream (now commonly termed as the East Asian jet), it starts to shift southward, which can be observed from the time–latitude variation of the zonal wind averaged from 110° to 130°E (Fig. 7). The shift does not go farther south of 30°N but becomes almost steady after day 3. To have a clearer view of the variation of the (subtropical) jet

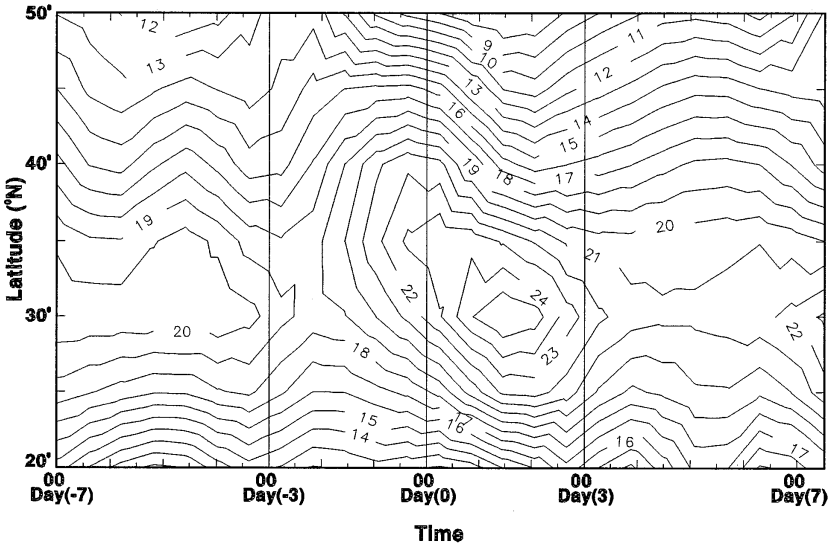

FIG. 7. The Hovmöller diagram of the 500-hPa zonal wind (m s^{-1}) averaged from 110° to 130°E of an NS.

core, the zonal component of the jet core is considered (Fig. 8). The region of 25°–35°N, 120°–140°E[1] is assigned as the region of jet core [smaller as compared to the region considered by Chang and Lau (1982), which is 20°–40°N, 100°–160°E]. It is clear that the jet core is strengthening from the minimum on around day −1 to a maximum on around day 2. The *secondary* intensification of the winds most evident at 200 and 300 hPa shortly after the NS (beyond day 3) is probably due to the upper-level return flow (feedback) of the local Hadley circulation (e.g., Chang and Lau 1982). To visualize the variation of the local Hadley cell, the vertical cross sections of the meridional circulations along 115°E averaged from day −3 to day −1 and day 1 to day 3 are investigated (Figs. 9a and 9b). The low-level invasion of the northerlies is consistent with the surface

[1] Note that the region of 110°–130°E is considered in the shift of the jet stream but it is 120°–140°E in considering the jet core variation. The former investigates the latitudinal shift of the jet stream, and the latter concerns the strength of the jet core.

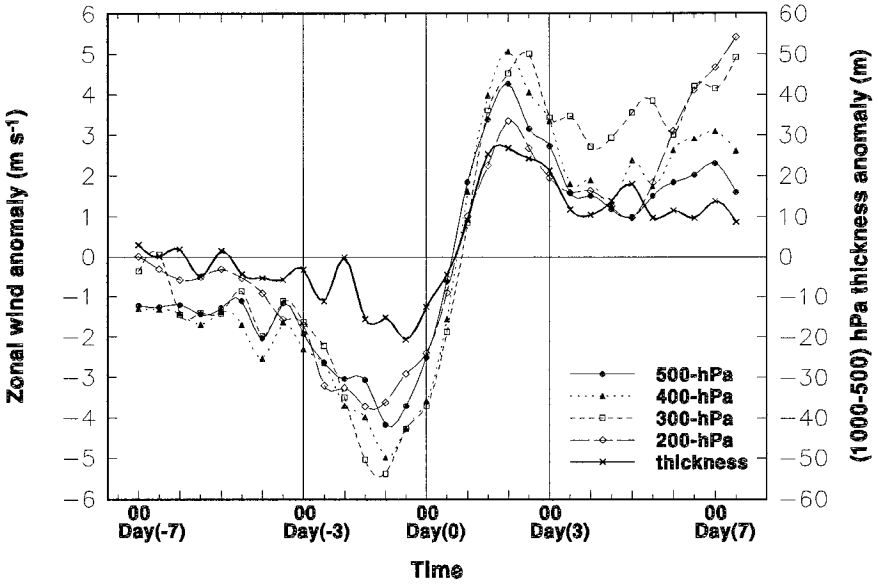

FIG. 8. The time variations of the zonal wind anomaly of the jet core 25°–35°N, 120°–140°E at different levels. Also shown is the 1000–500-hPa thickness anomaly difference of the belt 32.5°–35°N from 25° to 27.5°N averaged from 120° to 140°E.

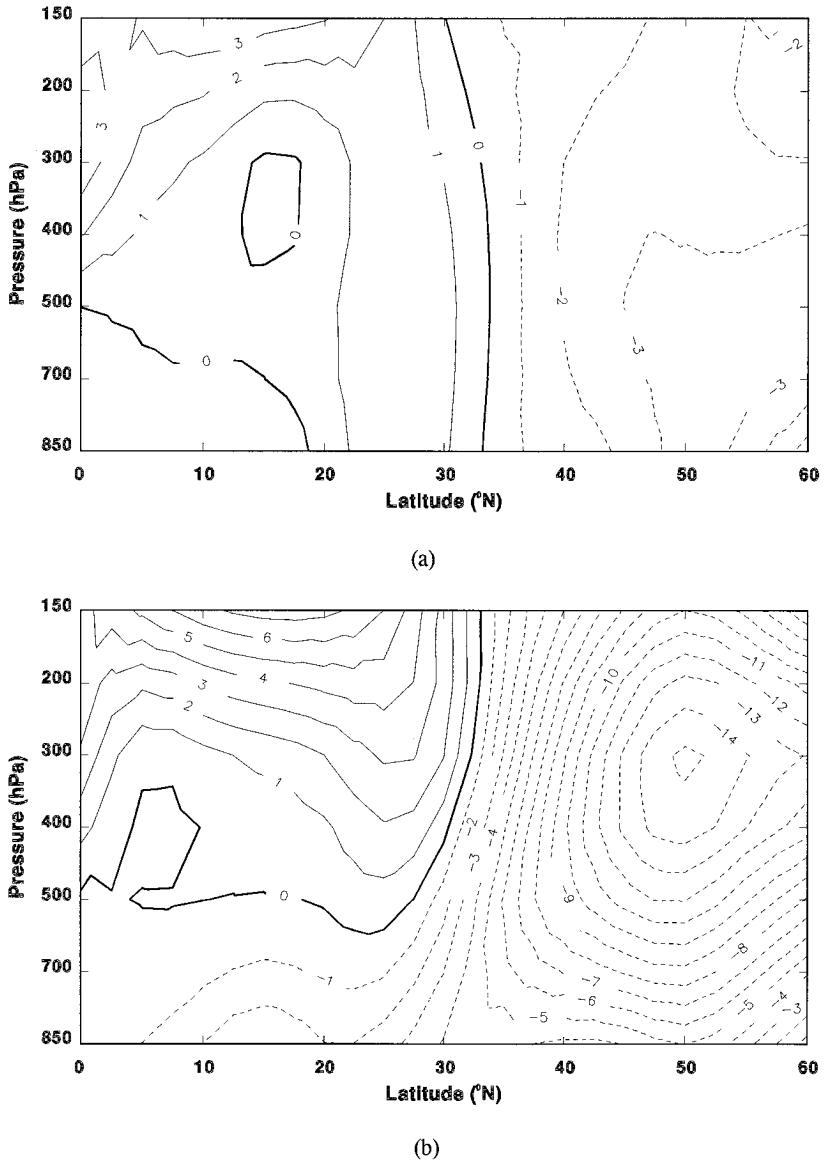

FIG. 9. The vertical cross section of the meridional wind (m s^{-1}) along 115°E averaged from (a) day −3 to day −1 and (b) day 1 to day 3.

northerly surge. Additionally, the strong southerlies above the northerlies layer reflects the intensification of the local Hadley cell after the NS (e.g., Ding and Xiao 1992). Evidently, the local Hadley cell is better defined after the NS.

To summarize, zonal winds at higher latitudes increase before an NS and are closely related to the propagation of a jet streak and the corresponding short wave (and also the development of the Siberia–Mongolia high; see next section). After that, the East Asian jet or the subtropical jet strengthens and attains a maximum on around day 2. In the upper troposphere, the jet increases further beyond day 3 because of the return flow associated with the surge from the equatorial region. We also observe the southward migration of the jet stream axis from around 40° to 30°N. As the axis of the jet stream represents the boundary of stronger temperature contrast, which in turn represents the boundary of the polar and tropical air masses, a cold outbreak is readily shown as a southward intrusion of the colder polar midlatitude air into the lower-latitude region.

Clearly, the above is quite different from that in the scenario given by Chang and Lau (1980). In the latter, a surface cold surge (NS) is induced when the intensity of the subtropical jet over the vicinity of Japan (thus called the East Asian jet stream) attains a maximum. In the present finding, the intensification of the subtropical jet *lags* the surge of the surface northerlies. However, the upper-level circulation is most meridional by around day 0, which is consistent with that on the surface.

Therefore, the disagreement in the timing of the maximum subtropical jet observed is not due to any difference in the definition of the timing of day 0 of the NS (or cold surge) as adapted by Chang et al. (1980). According to Bluestein (1992b), it is not entirely true that the migration/meandering of the jet stream is responsible for cold and warm anomalies at the surface. However, *the migration of cold and warm air mass is to some extent itself responsible for the meandering of the jet stream through the thermal wind relation.* In analogy to this, the subtropical jet is somehow responding to the NS (a large-scale north–south thermal exchange process) such that the strengthening (attaining a maximum) and the migration of the jet lag the surface surge. On the other hand, the passage of the polar jet and its subsequent convergence with the subtropical jet over the vicinity of Japan is related to the evolution of the Siberia–Mongolia high. Similarly, if an eastward migrating and intensifying subtropical jet is initially at a northern location (without any polar jet stream), the Siberia–Mongolia high can develop with similar dynamics as those found in the above results. The subtropical jet (or the East Asian jet) in this situation behaves as both causing and simultaneously responding to the NS. The timing of the maximum strength attained thus could be consistent with the surface outbreak. Nevertheless, the response of the jet to the feedback flow from the strengthening of the local Hadley cell is evident from the secondary strengthening of the jet core aloft.

d. Siberia–Mongolia high

The study of the evolution of the Siberia–Mongolia region is carried out by defining it as a spatially constant domain based on the position of the surface anticyclone. (Note that no apparent motion of the 1000-hPa Siberia–Mongolia anticyclone is observed.)

The position of the Siberia–Mongolia high as shown on the 1000-hPa geopotential height chart is a broad and not clearly defined region. Ding (1994) considered the domain of the Siberia–Mongolia high to be 40°–60°N, 77.5°–122.5°E, while Ding et al. (1991) assigned the smaller area of 42.5°–57.5°N, 80°–120°E. The latter suggested that the mean central core position (of five cases) of the Siberia–Mongolia high is located around (45°–55°N, 90°–105°E), which is quite similar to that in this study (see Fig. 2).

The time–height variations of the relative vorticity, geopotential height anomaly, potential temperature (with anomaly), horizontal divergence anomaly, and meridional and zonal wind anomalies associated with the NS from day −7 to day 7 with values taken daily at 0000 and 1200 UTC over the Siberia–Mongolia region are considered. We consider relative vorticity instead of absolute vorticity because a fixed region is considered and the passage of a short wave is more evident in terms of the variation of relative vorticity.

1) RELATIVE VORTICITY AND GEOPOTENTIAL HEIGHT ANOMALY

Passage of an upper short-wave trough (the cyclonic vorticity axis taken to represent the trough line) over the domain from day −3 to day 0 is evident from the strongest cyclonic vorticity (Fig. 10a) observed on around day −2 to day −1 at the 300-hPa level (which is the approximate height of the tropopause), with the largest decrease in geopotential height (Fig. 10b) occurring shortly before. The trough tilts westward with height, and the trough passage follows an upper ridge as shown from the large positive height anomaly on day −6. Also, an intensification of the lower-tropospheric high is observed below 700 hPa, which becomes strongest around day 0 (greater than 40 m). This is again consistent with the highest MSLP observed on day −1 (and the strong anticyclonic vorticity, see Fig. 10a) such that the height (or pressure) increases at the lower level first. The time difference in the intensification of the high between the surface and the lower troposphere (e.g., the 850-hPa level) is probably caused by stronger radiational cooling over the surface layer. On the whole, the above observations are consistent with the passage of the trough.

2) HORIZONTAL DIVERGENCE ANOMALY

The vertical field can be inferred from the horizontal divergence patterns. The insignificant divergence at 500–300 hPa on days −7 and −6 is consistent with the level(s) of nondivergence for a quiescent troposphere (Fig. 10c). Afterward, rising (sinking) motion occurs from around day −5 (day −3) to day −3 (day −3) in the midtroposphere such that divergence (convergence) aloft is coupled with convergence (divergence) near the surface. The maximum horizontal divergence anomaly at 850 hPa occurring on day 1 corresponds to the southward surge of the Siberia–Mongolia air mass associated with its breakdown such that the 850-hPa divergence is the strongest after a brief time of removal of air mass at the surface (on day 0). Low-level divergence after day −3 also shows that the Siberia–Mongolia high is intensifying. Wu and Chan (1995) have shown that large-scale northerlies occur on day 0 when considering the MSLP and surface vector winds, which is also consistent with the deep layer of divergence observed such that the Siberia–Mongolia high has significantly intensified by this time. The strong upper-level convergence between day −3 and day 0 is clearly related to the strong positive relative vorticity (Fig. 10a) and the negative height anomaly (Fig. 10b). In addition, it is obvious that the breakdown of the Siberia–Mongolia high is a lower-tropospheric feature and starts from the surface such that the strong low-level divergence is coupled with strongest convergence taking place below 500 hPa from day 0 to day 3 (that is, the deep convergence aloft is

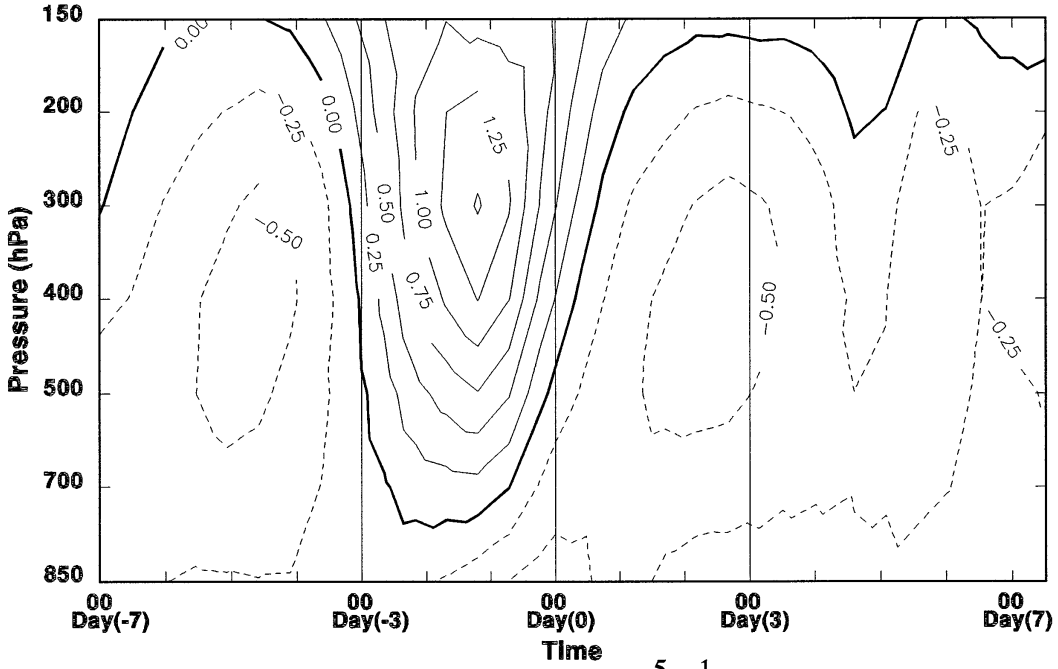

(a) relative vorticity (10^{-5} s^{-1})

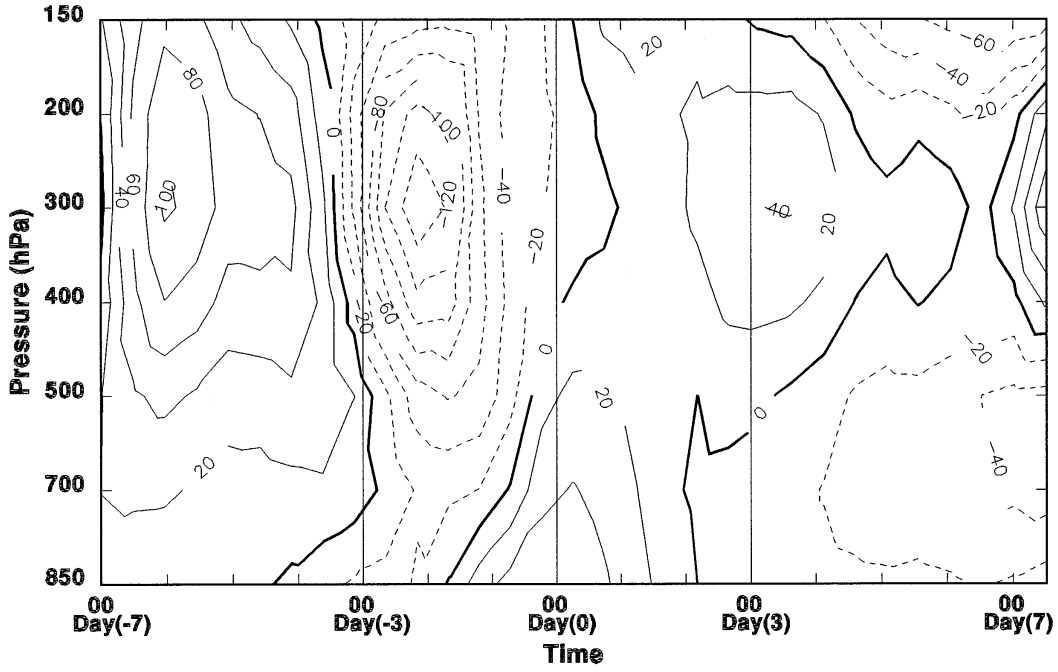

(b) geopotential height anomaly (m)

FIG. 10. The time variations of (a) relative vorticity, (b) geopotential height anomaly, (c) horizontal divergence anomaly, and (d) potential temperature with anomaly over the Siberia–Mongolia region.

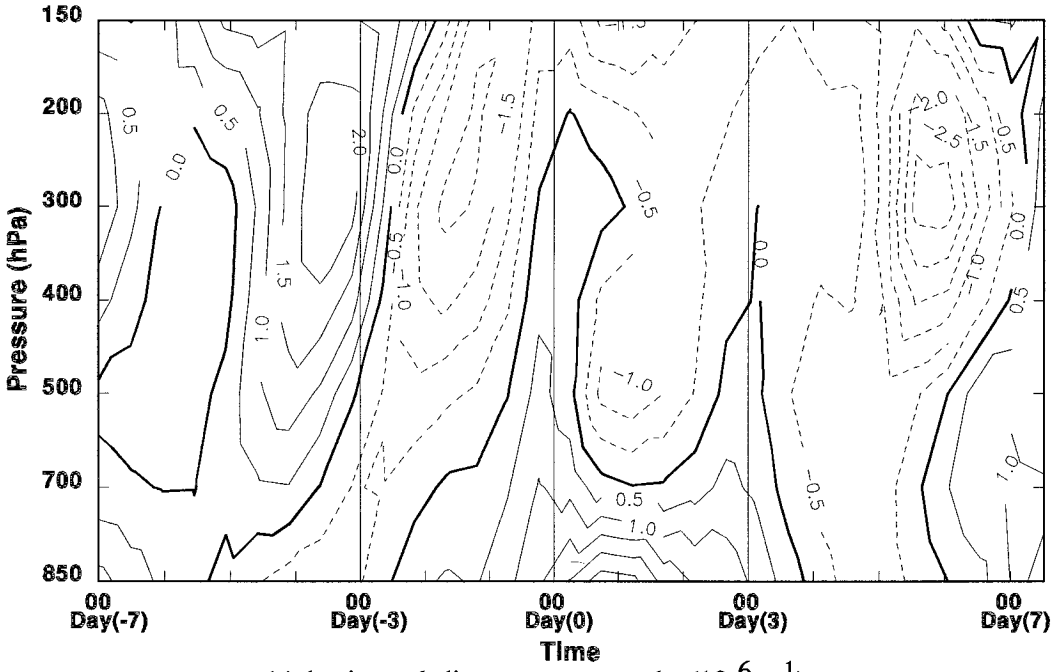

(c) horizontal divergence anomaly (10^{-6} s^{-1})

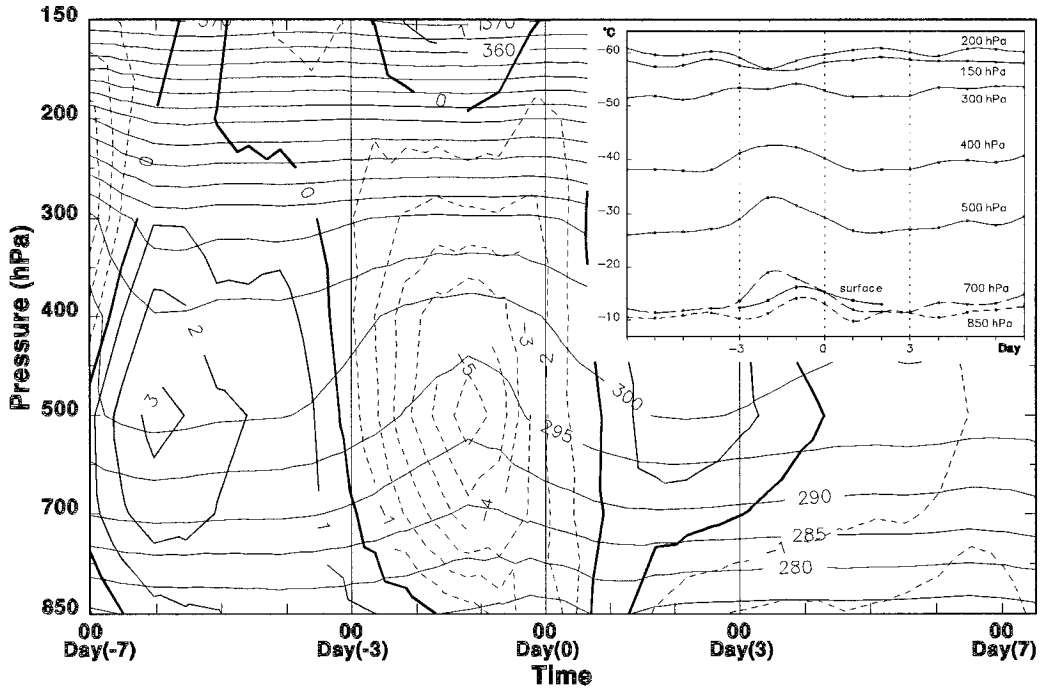

(d) potential temperature (solid) with anomaly (solid-dashed). (°K)

FIG. 10. (*Continued*)

induced from the low-level divergence rather than the dynamics of an upper wave).

3) Potential temperature

Figure 10d shows the time variations of the potential temperature anomaly and the temperature change at various pressure levels. It is clear that the most intense cooling takes place from day −3 to day −2 in the midtroposphere with a decrease of about 4–5 K per day (note that the cooling begins by day −6). Warming within the 850–300-hPa layers is observed after day −1, with the most significant warming occurring from day −1 to day 0.

From the temperature variations below 400 hPa, it is observed that the temperature drops and attains a minimum on around day −2 at pressure levels higher than 850 hPa first. The maximum temperature drops at the surface and at 850 hPa about 1 day later. This shows that the cooling starts from aloft and the main cause of the cooling is basically dynamically driven (probably due to the vertical motion induced adiabatic cooling). It can also be observed from the inset in Fig. 10d that the Siberia–Mongolia high has a temperature inversion below 850 hPa and the surface temperature is colder than at both 850 and 700 hPa after day 0 for a short period. The larger temperature drops at the surface than at the 850-hPa level are probably because radiative cooling at the surface enhances the degree of cooling so that inversion occurs.

Consider the (potential) temperature variations with the vertical wind field inferred from the horizontal divergence patterns. It is suggested that the cooling (warming) before (after) day −1 is due to the adiabatic cooling (warming) induced by rising (sinking) motions (note that a 4–5-K daily decrease in potential temperature at the midtroposphere is unlikely to be caused by adiabatic cooling). It can be seen that the strongest potential temperature change is at the midtroposphere, where the vertical motion associated with the trough evolution is the strongest. Hence, the cold-air mass passing over the Siberia–Mongolia region is intensifying (weakening) before (after) day −1. The largest negative potential temperature anomaly occurring at 500 hPa[2] by day −1 (note that it is prior to the maximum 850-hPa pressure anomaly) is consistent with the change over from the adiabatic-rising to -sinking motions such that the potential temperature increases after day −1 when the convergence aloft is at the maximum. Warming at the low-to-middle troposphere persisted to day 2 with the weakening of the Siberia–Mongolia high (see Fig. 10b), but it is observed from the divergence pattern that the breakdown of the lower-troposphere high system persisted until day 3 and day 4.

To a certian extent, it seems that adiabatic (vertical) processes play a significant role in the potential temperature variations in an NS within the midtroposphere, although no quantitative estimation in the diabatic processes such as the extent of radiative cooling and condensations has been considered. The vertical motion field will be inferred again by considering the quasigeostrophic forcing.

4) Quasigeostrophic forcing

According to the QG theory (e.g., the QG omega equation), rising (sinking) motion results from positive (negative) differential absolute vorticity advection and low-level warm (cold) advection[3] (e.g., Bluestein 1992a). It is observed that rising motion should be induced with the strong positive differential vorticity advection (Fig. 11a) before day −3. Strongest midtropospheric rising motion as inferred from the strongest divergence aloft (see Fig. 10c) occurs on day −4 concomitant with the positive differential absolute vorticity advection and warm advection (Fig. 11b) in the midtroposphere. Obviously, these features are inherent downstream of a short-wave trough aloft, and thus an upper short-wave trough is approaching the Siberia–Mongolia region. On day −2 (day −1), strong sinking motion in the midtroposphere (lower troposphere) should occur when the situation is reversed (i.e., negative differential vorticity advection coupled with cold advection underneath) as the trough is passing over. On the other hand, midtropospheric potential temperatures reach a minimum on day −2 and day −1 (see Fig. 10d), which can be explained in terms of the strong low-level horizontal and vertical (due to sinking of cold air) cold advection. The strongest subsidence induced at the midlevels from the most negative differential vorticity advection on day 0 (Fig. 11a) corresponds to the short period of deep divergence penetrating upward to 200 hPa, which in turn is associated with the strongest convergence at 300 hPa by day −1. These may be the first signs of the breakdown of the *intensifying* Siberia–Mongolia high. The weakening of the vorticity advection forcing on sinking motion and the strongest 850-hPa divergence again show that the strong 500-hPa convergence on day 1 should be caused by the lower-level divergence. From day 0 to day 3, a weakened differential absolute vorticity advection with low-level warm advection and low-level divergence is likely to be responsible for the breakdown of the low-level Siberia–Mongolia high.

[2] The fact that the minimum potential temperature anomaly occurs at the middle troposphere also suggests that the variation is due to adiabatic cooling such that vertical motion at the midlevel is expected to be most significant.

[3] The *geostrophic* advection is considered in the QG theory, and advection by the actual wind is used in the above discussion.

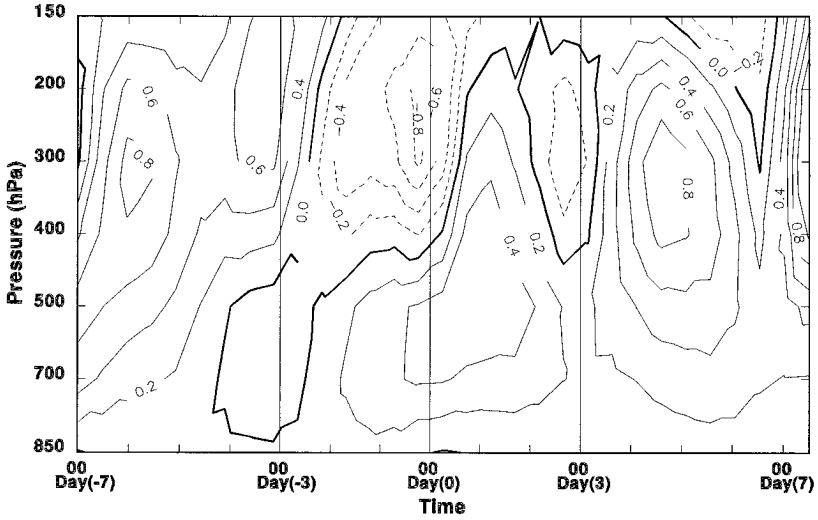

(a) absolute vorticity advection (10^{-10} s^{-2})

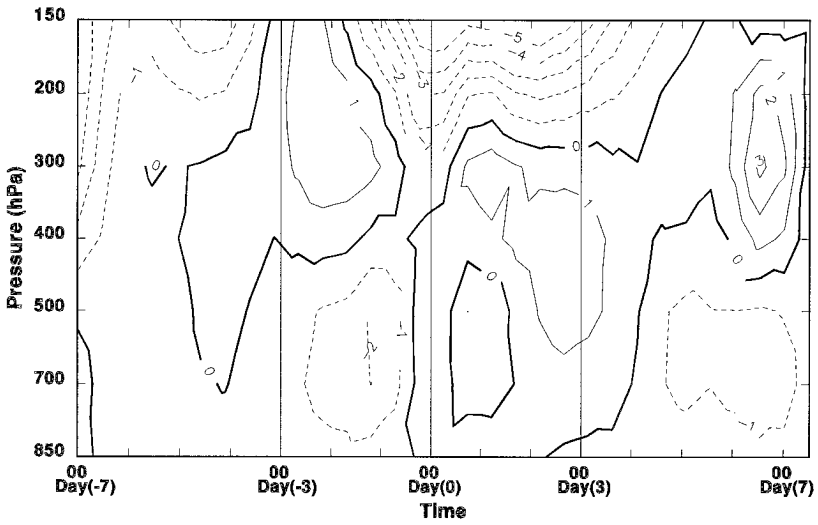

(b) potential temperature advection (10^{-5} °K s^{-1})

FIG. 11. As in Fig. 10 except for advection of (a) absolute vorticity and (b) potential temperature.

According to Boyle and Chen (1978), the low-level anticyclonic circulation development over China in a cold outbreak (e.g., the southward intrusion of the 850-hPa high) is the result of upper-level vorticity advection and lower-level cold advection and should be distinguished with the semipermanent wintertime Siberia–Mongolia high (i.e., as the one observed in the normal condition). This is consistent with the above observation in the transient nature of the development (intensification) of the Siberia–Mongolia high. Furthermore, the horizontal advection of (absolute) vorticity and potential temperature does have a close relationship with the transient evolution of the Siberia–Mongolia high.

5) BRIEF SUMMARY

The above results show that the Siberia–Mongolia (cold) air mass (and the migrating cold air mass) is accumulating before day −3, probably by the forced adiabatic cooling at the midlevels due to the intense divergence aloft associated with the shortwave trough passage. The Siberia–Mongolia high becomes further strengthened (in terms of geopotential height) at lower levels because of the subsidence (due to the sinking of *cold* air) from higher levels afterward. Besides the investigation by Xie et al. (1992), the importance of the ascending cooling in intensifying the cold dome has also been stressed by Qiu (1988). The midlevel sinking mo-

tion induced from the strong 300-hPa convergence on day −2 and day −1 may in turn induce a triggering mechanism for the breakdown of the Siberia–Mongolia high later. On the other hand, the low-level divergence associated with the breakdown of the high may prompt the midtropospheric sinking motion and the midlevel convergence. Up to now, whether the breakdown of the Siberia–Mongolia high is caused by the intense pressure/height gradient or the downward push associated with the sinking motion (due to convergence aloft) is not completely clear. The changeover between rising (initially) and sinking (afterward) motion can also be understood as the passage of trough aloft. In a baroclinic wave system, the lower troposphere consists of rising (sinking) motion downstream (upstream) of the trough (e.g., Palmen and Newton 1969).

To summarize, the evolution of the lower-tropospheric Siberia–Mongolia high is a dynamic process that can be described in terms of the QG theory and the nature of a developing/unstable baroclinic wave system. The change in various meteorological fields such as potential temperature on around day −2 is related to the passing of a short-wave trough. The approach (departure) of the polar jet and short wave toward (from) the Siberia–Mongolia region represents the building up (decay) stage of the Siberia–Mongolia high. Rising motion downstream from an approaching trough induces cooling effect at the midlevels. It is suggested that the lower-tropospheric height is intensifying due to 1) the subsidence of the ''cooled'' air (the adiabatic subsidence warming has little effect on the height increase) associated with the passing of the trough and jet streak aloft and 2) the low-level radiational cooling effect. When the subsidence aloft is the strongest, the Siberia–Mongolia high collapses and an NS is induced with a strong lower-level divergence, which thereby enhances the sinking motion. Some important features prior to the outbreak at day −1 and day −2 are 1) the lowest potential temperature at midlevels, which starts to rise afterward; 2) large cyclonic (relative) vorticity associated with strong convergence and subsidence aloft; 3) the largest differential (absolute) vorticity advection; 4) the largest low-level cold advection; and 5) stronger westerly and southerly anomalies aloft. On the other hand, the characteristics of the Siberia–Mongolia region during and after the NS are 1) a rise in potential temperature in the lower midtroposphere, 2) strong low-level divergence with the convergence center at midlevel (500 hPa, say), 3) replacement of cyclonic vorticity by anticyclonic vorticity, 4) strong northerlies anomaly aloft, and 5) the weakest zonal flow aloft representing the decrease in the degree of baroclinicity.

e. Summary

The evolution of the intense Siberia–Mongolia high responsible for an NS is related to an eastward passage/propagation of the polar jet streak migrated from the west of Lake Balkhash and the corresponding short-wave trough behind, which in turn can be explained by the QG theory (in terms of absolute vorticity and potential temperature advection). Based on the observations in the QG forcing patterns, a development of the Siberia–Mongolia high is suggested. As inferred from the QG forcing and the relative positions of the trough and polar jet stream, the development of the Siberia–Mongolia high is depicted schematically in Fig. 12, which shows the relative positions and the corresponding effects of the polar jet streak, the short-wave trough, and the cold tongue at different stages of an NS with respect to the surface Siberia–Mongolia high. In the accumulating or intensifying stage, the ascending branch of the thermally indirect transverse circulation associated with the polar jet streak couples with the secondary circulation downstream of the trough in a developing baroclinic (short) wave to give the intense adiabatic cooling over the Siberia–Mongolia region. The lifting by the jet streak causes low-level convergence such that a synoptic-scale inflow into the Siberia–Mongolia vicinity is induced, resulting in the surface warming over most parts of China before an NS (see Wu and Chan 1995). Apart from the adiabatic cooling, the horizontal advection accompanying the migrating cold-air mass (or cold tongue) and the radiative cooling at lower troposphere also cause a large decrease in potential temperature and the strengthening of the cold dome over the Siberia–Mongolia vicinity. Prior to its breakdown, the Siberia–Mongolia high further intensified because of the strong subsidence induced when the shortwave passed over and the jet streak departed. At the same time the cold dome (at midlevels) is the coldest with the low-level geopotential height of the Siberia–Mongolia high attaining a maximum, and thereafter an outburst starts at the lower troposphere. The outpouring of lower-tropospheric air induces even stronger sinking motion and low-level horizontal divergence so that the cold dome breakdown with midlevel convergence results. The NS ends with the weakening of the Siberia–Mongolia high and the baroclinic (short) wave system. It should be noted that the above picture of the development of the NS is only a suggestion based on the observations. Further investigation is needed to study the schematic development.

The low-level features after the outbreak of the NS are the large-scale meridional flow accompanied by strong cold advection and a southward push of pressure/height contours. The southward migration of the Siberia–Mongolia air mass is best revealed from the southward and anticyclonic-turning track of the 850-hPa-high height center, which resembles the trajectory of cold air behind a cold front. The subtropical (or southern) jet at the southern flank of the Tibetan Plateau strengthens in response to (or associated with) the cold outbreak after it has merged with the polar jet into a single major jet over the vicinity of Japan. As the cold air accompanying the NS surges southward and meets the warmer tropical

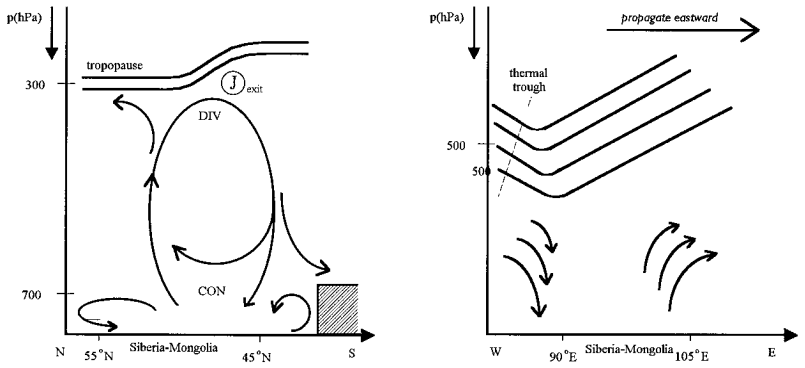

(a) intensification/building up of the Siberia-Mongolia high

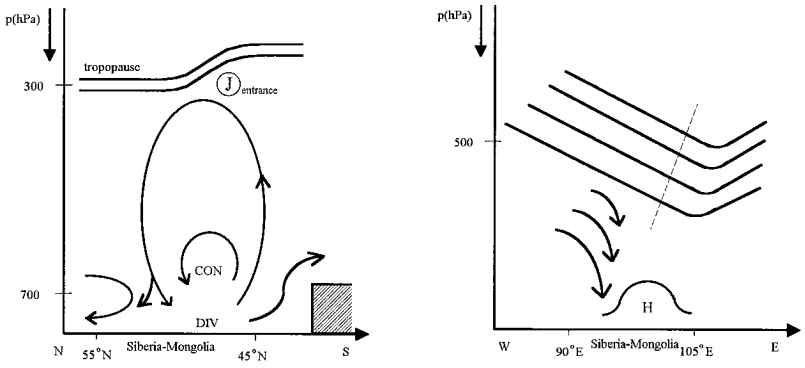

(b) outbreak/breaking-down of the Siberia-Mongolia high

FIG. 12. Schematic showing the evolution of the Siberia–Mongolia high in an NS at the stages of (a) intensification and (b) outbreak. Left panels show the transverse circulation associated with the jet at the (a) exit and (b) entrance regions. Right panels present the secondary circulation associated with the passage of the height and thermal trough when (a) the short wave is heading toward and (b) away from the Siberia–Mongolia region.

air mass (the warm spell before NS has also enhanced the temperature contrast), the baroclinicity aloft is enhanced over the vicinity of Japan and the (East Asian) jet strengthens according to the thermal wind relation. Meanwhile the short-wave trough has merged with the long-wave trough, which deepens further. At the same time, the NS occurs (large-scale low-level meridional flow) when the flow aloft is most meridional such that the zonal index is the lowest.

The response at the lower-latitude region to the large-scale lower-level meridional flows is the enhancement of the local Hadley cell. This can be observed from the fact that the local Hadley cell is more well defined after the NS, as revealed from the meridional flow patterns. The return flow of the local Hadley cell after the NS causes a secondary strengthening to the East Asian jet stream at upper levels. The situation is depicted in Fig. 13 showing the evolution of the local Hadley cell.

3. Easterly surge

a. Lower-tropospheric features

1) 1000-hPa SYNOPTIC CHART

From the 1000-hPa synoptic chart, the high center over the Dahingganling is a breakoff from the Siberia–Mongolia high (Fig. 14) (for convenience, the high center is termed the Dahingganling high throughout its development). The most evident splitting begins on day -2 (at 1200 UTC from a 12-h chart) when the strength of the Siberia–Mongolia high is decreasing. Thereafter, the Dahingganling high migrates southeastward quickly and independently, while the quasi-stationary Siberia–Mongolia high gradually intensifies to the normal value. Finally, the strength of the Dahingganling high decreases along its eastward track.

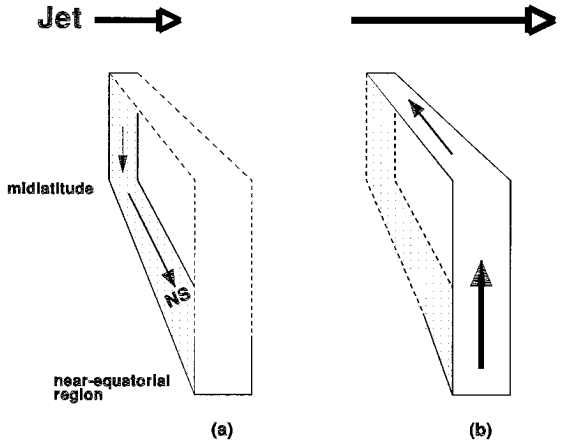

FIG. 13. The schematic showing the evolution of the Hadley cell (a) before and (b) after an NS. The arrows within the Hadley cell in (a) and (b) represent the large-scale meridional flow (NS) and the return flow, respectively. The jet stream is further strengthened in (b).

2) NORTH–SOUTH CONTRAST

The north–south thickness anomaly contrast decreases during the splitting of the Siberia–Mongolia high into the Dahingganling high until day 1 in the case of ES, which is different from that of the NS (Fig. 15). The thickness difference anomaly is generally negative during the ES episode, and the decrease starts from a value close to normal showing that the lowering of the north–south potential energy contrast is unlikely to be caused by a meridional temperature gradient. Similarly, the north–south pressure/height gradient at 1000 hPa rises from day −2 to day 0 (i.e., during the eastward migration of the 1000-hPa high height center) in an ES (Fig. 16).

3) 850-hPa FEATURES

A broader-scale 850-hPa high is located over the vicinity of the East China Sea and the China landmass on day −1 (Fig. 17). Winds at 850 hPa are quite close to geostrophic in terms of their direction over the central China plain, and the anticyclonic flow centers can be

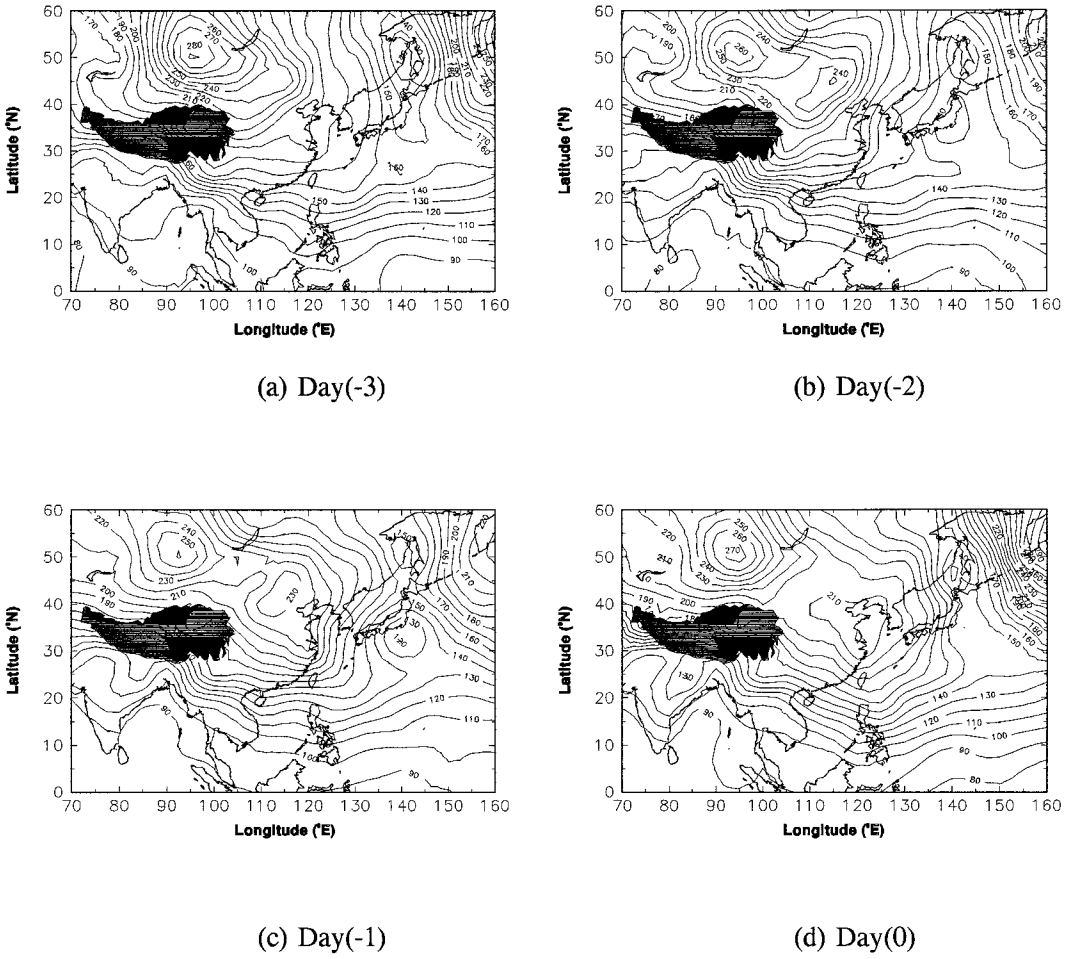

FIG. 14. The 1000-hPa geopotential heights (m) of an ES.

identified between day −1 and day 1. Clearly, the lower-tropospheric Dahingganling high tilts southward[4] with height such that its center at 1000 hPa (also the MSLP high center) lies north and west of that at 850 hPa. The high also migrates slightly faster at the surface than at the 1000- and 850-hPa levels.

Over the region of northern China, the region of 24-h potential temperature rise at 850 hPa between day −1 to day 1 is quite consistent with that of the 1000-hPa Dahingganling high, despite the occurrence of cold advection[5] (Fig. 18). This suggests that the subsidence-induced warming of the Dahingganling high is the main cause of the temperature rise, which overwhelms the effect of cold advection. The effect of subsidence may transform the Dahingganling high into a warm high.

On the other hand, the temperature drop over south China on day −1 is because of the northerly flow, that is, cold advection. From day 0 to day 2, it is obvious that the rise is due to the southerly and onshore flow associated with the eastward passage of the high over the Yellow Sea. On the whole, the temperature change at 850 hPa over the south China region is consistent with that at the surface (Wu and Chan 1995).

4) SUMMARY

The fundamental character of the ES in the lower troposphere is the southeastward migration of the Dahingganling high, which is split out from the semipermanent Siberia–Mongolia high. The Siberia–Mongolia high in the ES is weaker than in the case of NS, probably because of the splitting. Another interpretation is that the splitting results from a nonintensifying Siberia–Mongolia high. In other words, an intensifying Siberia–Mongolia high is unlikely to split away to induce an ES. During the southeastward migration, the Dahingganling high transforms into a warmer shallow high center because of subsidence-induced warming and the diabatic heating of landmass so that the low-level temperature increases near the vicinity of the high.

[4] The center of the high at 850 hPa is better observed from the 850-hPa anticyclonic flow centers in Fig. 16.

[5] The temperature advection distribution will not be shown, but the advection variation can be inferred from the wind flow and the potential temperature distribution.

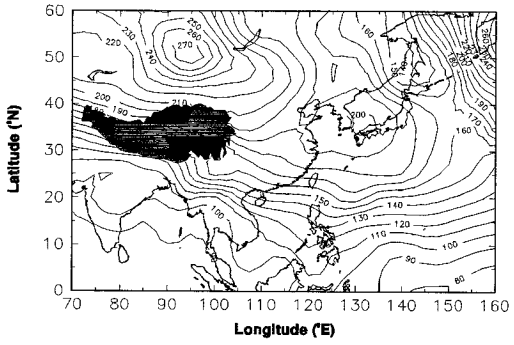

(e) Day(1)

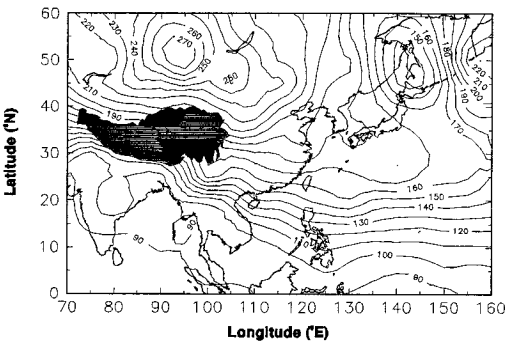

(f) Day(2)

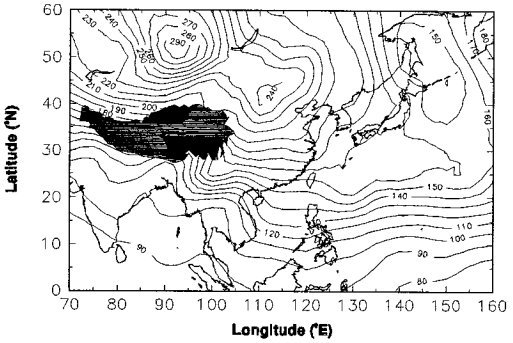

(g) Day(3)

FIG. 14. (*Continued*)

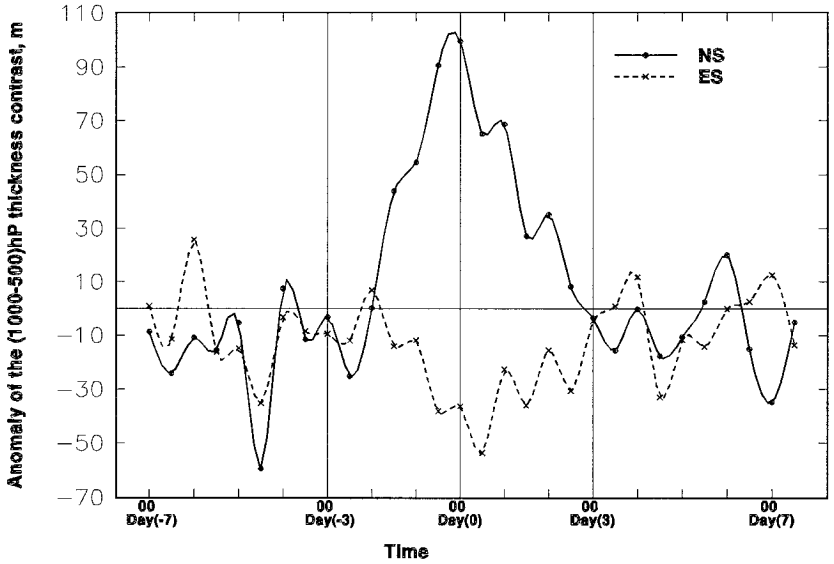

FIG. 15. Time variation of the north–south 1000–500-hPa thickness contrast anomaly of an ES and an NS. North–south contrast is defined as the difference of the belt 40°–50°N from that of 15°–25°N within 90°–130°N.

b. Zonal index and Hovmöller diagram

The time variation of the zonal index has been considered in the study of the NS. From Fig. 4, it is observed that the upper circulation becomes more zonal during an ES and the eastward migration of the low-level Dahingganling high may be related to the zonal upper-flow steering. The most abrupt increase of the index at day −2 (also at 1200 UTC) is also consistent with the splitting of the lower-tropospheric Siberia–Mongolia high (at 1000 hPa say). The index decreases by day 1 when the lower-tropospheric Dahingganling high is over the Yellow Sea. As with the NS, an ES represents a kind of large-scale flow adjustment. Therefore, an ES can be taken as an event of increasing zonal index at the 500-hPa level.

From the Hovmöller diagram (Fig. 19), the passage of a 500-hPa (height) ridge is observed. Obviously, the passage of a ridge instead of a trough will cause different variations to the Siberia–Mongolia high. The passage of the ridge aloft over the Siberia–Mongolia region may be a reason for the splitting of the Siberia–Mongolia

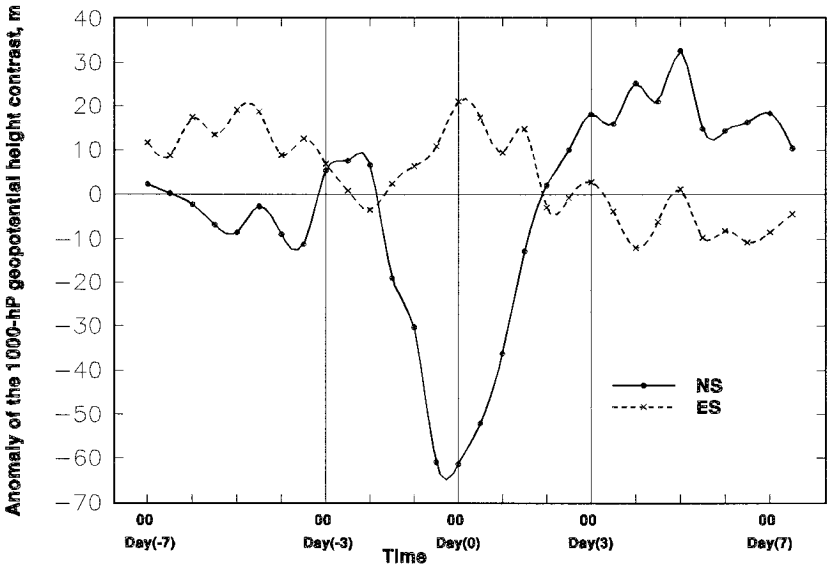

FIG. 16. As in Fig. 15 except for 1000-hPa geopotential height anomaly (m).

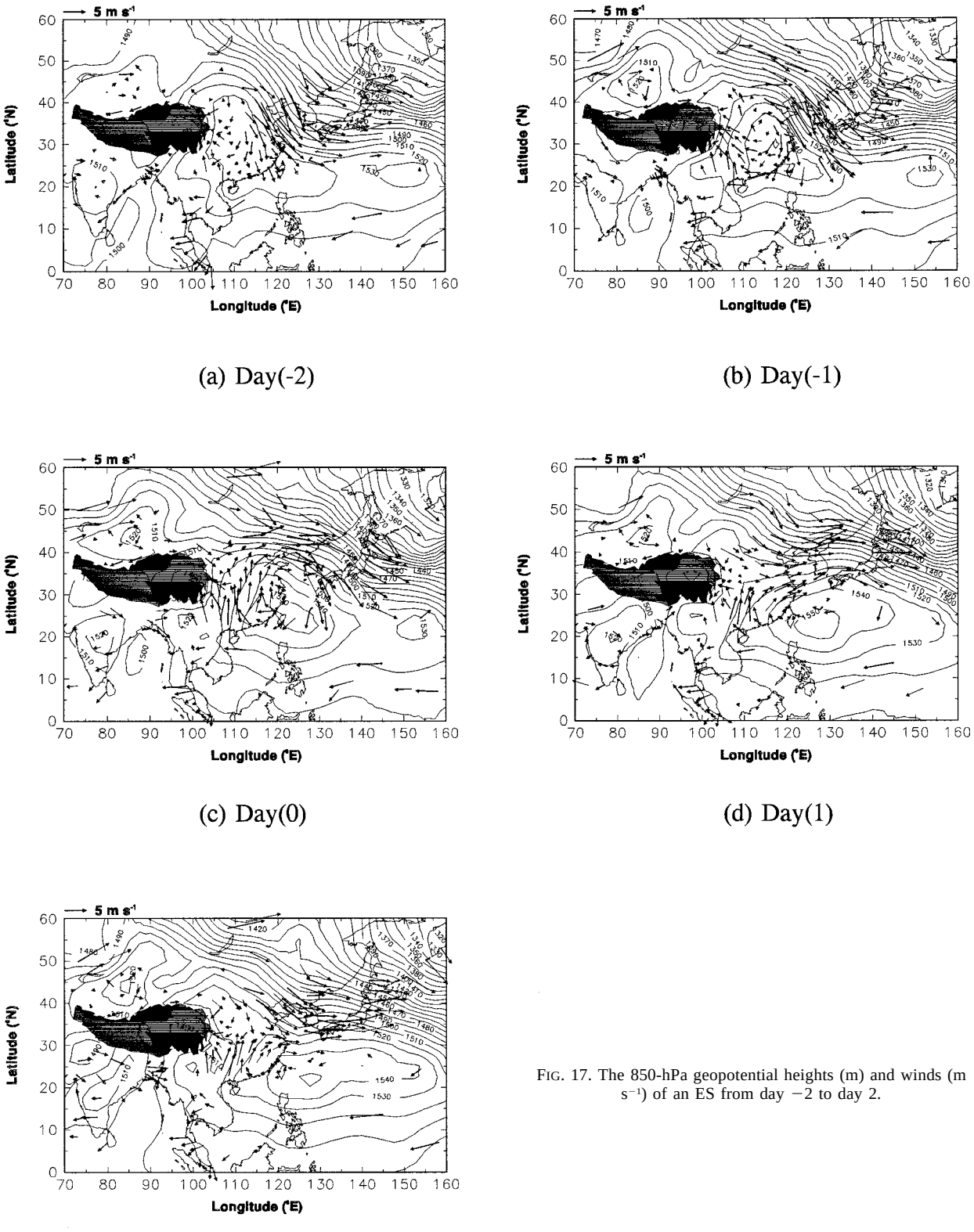

FIG. 17. The 850-hPa geopotential heights (m) and winds (m s^{-1}) of an ES from day −2 to day 2.

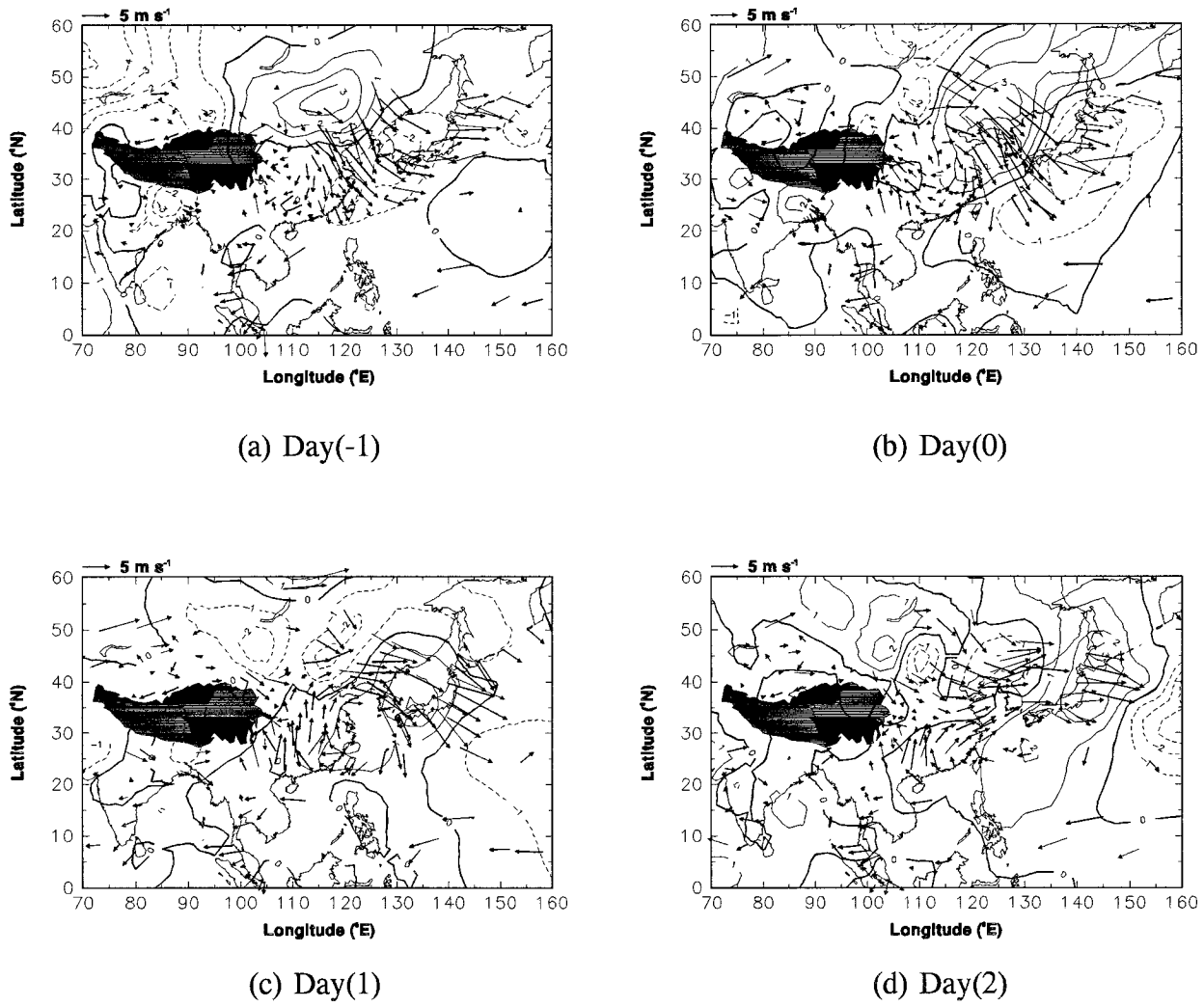

FIG. 18. The 24-h potential temperature change and wind distribution (at 1 day before) of an ES from day −1 to day 2 at 850 hPa.

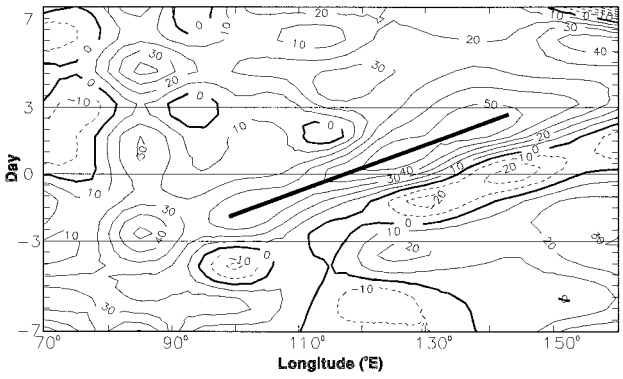

FIG. 19. The Hovmöller diagram of the 500-hPa geopotential height anomaly (m) of an ES. The solid line defines the passage of the ridge.

high on day −2 and the subsequent eastward motion of Dahingganling high.

c. Jet stream

In an ES, the subtropical jet is seen to be quite stationary and located at the mean position (i.e., 30°N) (not shown). The strength of the jet reaches the maximum on around day −2, that is, before the ES, but is weakening afterward with no apparent latitudinal shift of the jet stream observed. It is more clear from the variation of the jet core 500-hPa zonal wind anomaly (Fig. 20) that the jet stream is weakening in an ES, which is opposite in the NS. Furthermore, the below-normal jet core is quite steady for a brief period after day 2 and day 3, until day 5.

Barotropic instability may be associated with an ES such that the zonal kinetic energy of the upper westerlies is converted into the kinetic energy of the disturbance

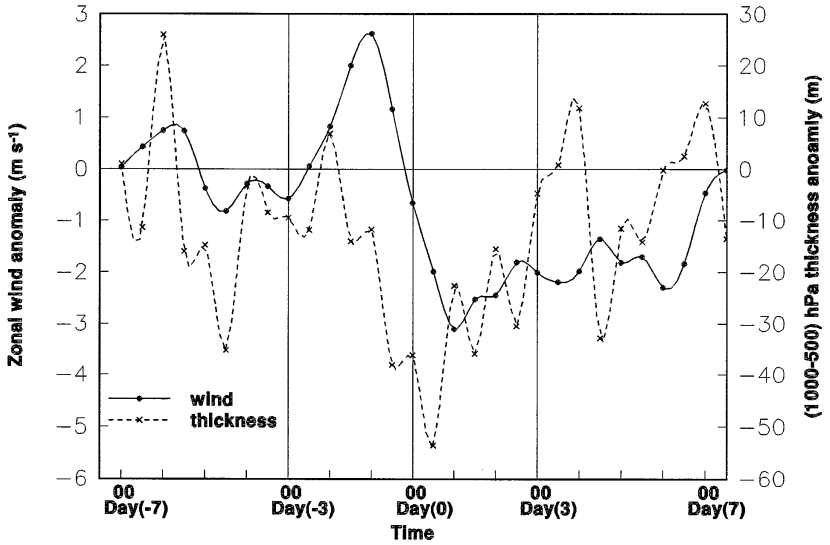

FIG. 20. Time variation of the 500-hPa zonal wind anomaly (m s^{-1}) of the jet core 25°–35°N, 120°–140°E and the anomaly of the north–south 1000–500-hPa thickness contrast (m) (see Fig. 14 for the definition of the north–south contrast) of an ES.

of the ES such as the migration of the surface Dahingganling high. Since the zonal kinetic energy as inferred from the zonal flows of the jet core is seen to decrease from day −1, the conversion of the kinetic energy into either the potential energy or the kinetic energy of the eddies/disturbance warrants further investigation. To do this, the average of 500-hPa zonal flow from 120° to 140°E is taken as the basic zonal current. This region is considered because it is the jet core region and the assumption of zonal basic current is most appropriate for its stronger zonal speed. It can be observed from Fig. 21 that the gradient of absolute vorticity vanishes between 0000 and 1200 UTC on day −1 at around 40°N, that is, at the cyclonic-shear side of the jet streak. The maximum gradient at around 30°–32.5°N on day −1 is consistent with the maximum strength of the jet core, which weakens thereafter. The decrease of the 1000–500-hPa thickness anomaly across the jet core with the zonal wind is also consistent with the thermal wind relation (see Fig. 20). Further, the decrease in the jet zonal kinetic energy is unlikely to result in an increase of the north–south potential energy because the north–south thickness contrast is decreasing.

d. Dahingganling high

The Dahingganling high is a shallow system that is observed below 850 hPa and is well observed/defined from day −2 at the 1000-hPa level and the surface after its split from the Siberia–Mongolia high until day 1. To investigate the evolution of the high along its track, a 10° longitude by 10° latitude square is used to define the center of the 1000-hPa Dahingganling high and the regions from day −3 to day 2 as shown in Fig. 22. (Note that the Dahingganling high at day −3 can be regarded as the Siberia–Mongolia high.)

It is observed that temperature inversion between the surface and 850 hPa only occurs at day −3 and day −2 (Fig. 23). When the high is located farther south and east after day −2, no inversion is observed, showing that the cold-core nature of the high has largely disappeared.

e. Summary

The eastward migration of a surface high pressure system breaking off from the Siberia–Mongolia high leads to an ES event. When the high is over the Yellow Sea, ridging along the east and south China coasts occurs, with easterlies surging along the east China coast and resulting in the strengthening in surface easterlies along the coast. Associated with its eastward path, the Dahingganling high undergoes significant transformation.

The Siberia–Mongolia high during an ES is weak, and the north–south thermal contrast decreases after its split. Therefore, the cause of the ES is unlikely to be the thermal contrast as in the case of NS. On the other hand, the breakoff of the Siberia–Mongolia high is related to the forcing of the ridge passing aloft. The evolution of an ES is schematically depicted in Fig. 24.

4. Conclusions

The two types of winter monsoon surges, ES and NS, are shown to have very different characteristics, and both of them represent a well-defined event taking place in Asia during wintertime. An evident lower-tropo-

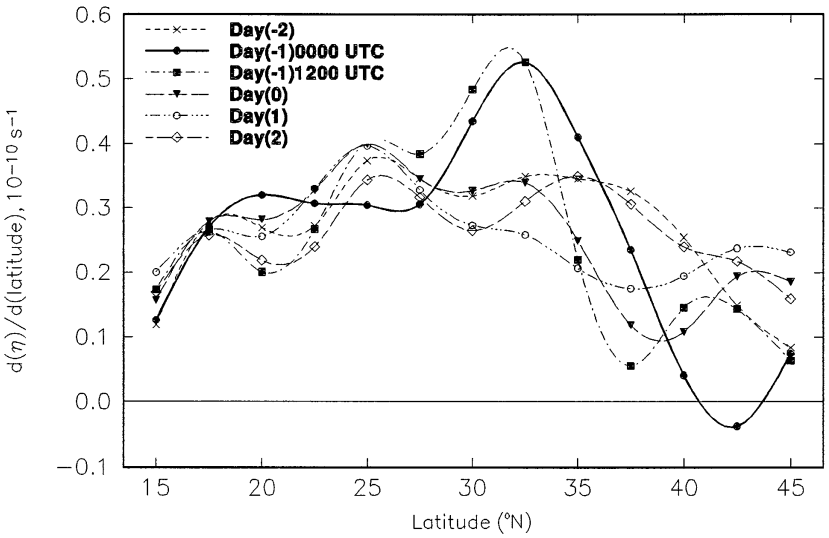

FIG. 21. The 500-hPa meridional absolute vorticity gradient ($\times 10^{10}$ s^{-1} deg^{-1}) from 120° to 140°E. Daily values are used except in day −1 of which 0000 and 1200 UTC are shown.

spheric feature associated with the ES is the eastward migration of a surface high pressure center, resulting in the strengthening of easterlies along the east to south China coast. The southward intrusion of cold air mass sweeping over most parts of China and the associated abrupt temperature drops and strengthening of northerlies are the characteristic features of an NS in the lower troposphere. Whether an ES or NS occurs depends on the strength and evolution of the Siberia–Mongolia high, the passage of a wave aloft, and the associated jet stream. The following summarizes and compares the processes of the NS and ES events.

The Siberia–Mongolia high undergoes the intensification, breakdown, and decay stages in an NS event with the outbreak occurring during its breakdown. It is suggested that the intensification of the Siberia–Mongolia high is related to the eastward passage of the polar jet streak that migrates from west of Lake Balkhash and the corresponding upstream short-wave trough. When the jet streak is approaching to the Siberia–Mongolia region, the ascending northern branch of the associated transverse circulation is coupled with the secondary circulation downstream of the short-wave trough to set up an intense adiabatic cooling. The arrival of the cold air mass (cold tongue) together with radiative cooling at the surface further intensifies the cold dome. In the mean time, the Siberia–Mongolia high attains a maximum when strong subsidence is induced by the passing over of the short wave and an outburst is initiated with the breakdown of the Siberia–Mongolia high. The outbreak or the breakdown of the Siberia–Mongolia high is accompanied with the southward (equatorward) intrusion of the cold air mass in the lower troposphere and a subsequent weakening of the high.

The large-scale meridional flow represents a cold front passage and is accompanied with strong cold advection and a southward push of pressure/height con-

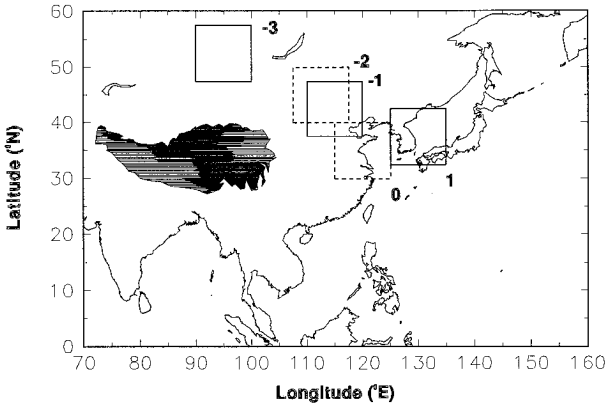

FIG. 22. The location of the Dahingganling high from day −3 to day 1 of an ES.

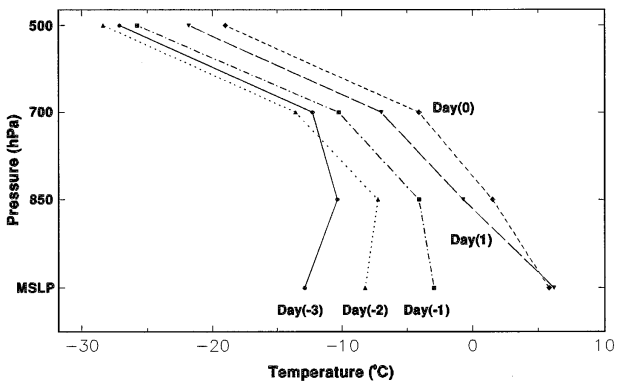

FIG. 23. Vertical profile of the temperature (°C) of the Dahingganling high at different times (day −3 to day 1) in an ES.

TABLE 1. Summary of the upper-level features associated with the ES and the NS.

Parameters	ES	NS
Zonal index	Increasing	Minimum at the outbreak and increasing during the NS
Upper wave passage	Ridge passage	Trough passage
Jet stream	Strength decreasing	Polar jet passage, merge with the subtropical jet, and intensify
Height system	Eastward migration of a high breakoff from the Siberia–Mongolia high at the 1000-hPa level	Southward migration of 850-hPa high center along the eastern flank of the Tibetan Plateau
North–south thermal contrast	Decreasing after the breakoff of the Siberia–Mongolia high and attaining a minimum just after the ES	Maximum during the cold outbreak and decreasing during the surge
Siberia–Mongolia high	1) Weaker than normal; 2) warmer than normal	1) Maximum strength before the cold outbreak; 2) coldest before the cold outbreak

tours. The southward migration of the Siberia–Mongolia air mass can be observed from the movement of the 850-hPa high center around the eastern flank of the Tibetan Plateau, which resembles the trajectory of the cold air behind the cold front. The response at the lower-latitude region to these large-scale lower-level meridional flows is the enhancement of the local Hadley cell such that the easterlies (westerlies) aloft are strengthened during (after) the NS.

In an ES, the Siberia–Mongolia high is not very intense and does not undergo a significant intensification. Instead, a surface high pressure center (the Dahingganling high) breaks away from it and subsequently migrates eastward. The surge of easterlies affects regions along the east and south China coast when the Dahingganling high is over the Yellow Sea, with the formation of pressure ridging along the coast. The splitting of the Siberia–Mongolia high is associated with the passage of an upper ridge and an increase in the zonal index. The characters of the ES can be better revealed from its differences with those of the NS (Table 1).

To summarize, this study attempts to find out the characteristics of the ES and the NS. Significant differences between the two types of surges are readily observed. One of the evident differences between the ES and the NS is the different trend of the time variation of the zonal index. In addition, the passage of ridge and trough aloft associated with the ES and the NS, respectively, is another pronounced contrast between the two types of surge. Moreover, the variations of the jet stream and north–south thermal contrast are different for the ES and the NS. Finally, it is suggested that the features found can be utilized for forecasting upon further investigation. For example, increase in the zonal index and eastward passage of an upper ridge over the

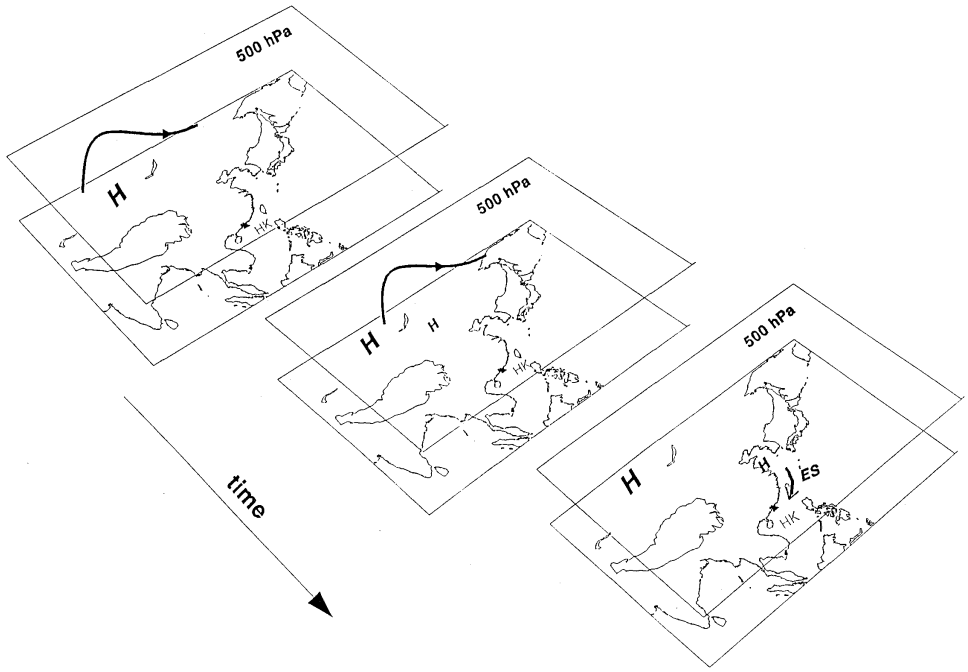

FIG. 24. Schematic showing the event of an ES. Passage of ridge aloft and splitting of the Siberia–Mongolia high are shown.

Siberia–Mongolia region can be forecasting criteria for the ES. Similarly, the passage of a trough over Lake Baikal is a method for the forecasting of the arrival of the NS (cold surge), which is, in fact, currently used by the ROHK.

5. Concluding remarks

The most deficient aspect of the present study is the lack of vertical velocity data so that the vertical motion field cannot be investigated in detail. For example, vertical motion over the Siberia–Mongolia region can only be inferred from the divergence pattern and QG forcing when the errors in computing the divergence may be quite large (e.g., Bluestein 1992a) and the assumption of direct response to QG forcing may not be completely true. The insufficient temperature data at 1000 hPa also prohibit the investigation of the gravity wave nature associated with the NS and the mass/momentum propagation along the coastal line in the ES. Such investigations will be the subject of a subsequent study.

Acknowledgments. The authors would like to thank the Royal Observatory of Hong Kong for providing all the data used in this study. The help in computer programming by Mr. K. W. Ngan and Mr. C. H. So is also gratefully appreciated. In addition, the efforts of Mr. C. K. Fong in initiating the data extraction procedure are gratefully acknowledged. Detailed comments from one of the reviewers are also much appreciated. The Computing Services Center of the City University of Hong Kong provided the necessary computer resources.

The first author is a recipient of a research studentship provided by the City University of Hong Kong. Finally, this research is partially supported by the Research Grants Council of the Universities Committee of Hong Kong Grant 904074.

REFERENCES

Bao, C., Ed., 1987: *Synoptic Meteorology in China.* China Ocean Press, 269 pp.

Bluestein, H. B., 1992a: *Principles of Kinematics and Dynamics.* Vol. I, *Synoptic–Dynamic Meteorology in Midlatitudes,* Oxford University Press, 429 pp.

——, 1992b: *Observations and Theory of Weather Systems.* Vol. II, *Synoptic–Dynamic Meteorology in Midlatitudes,* Oxford University Press, 594 pp.

Boyle, J. S., and T.-J. Chen, 1978: Synoptic aspects of the wintertime east Asian monsoon. *Monsoon Meteorology,* C. P. Chang and T. N. Krishnamurti, Eds., Oxford University Press, 125–160.

Chang, C. P., and K. M. Lau, 1980: Northeastly cold surges and near-equatorial disturbances over the winter MONEX area during December 1974. Part II: Planetary-scale aspects. *Mon. Wea. Rev.,* **108,** 298–312.

——, and ——, 1982: Short-term planetary-scale interactions over the tropics and midlatitudes during northern winter. Part I: Contrasts between active and inactive periods. *Mon. Wea. Rev.,* **110,** 933–946.

Chu, E. W. K., 1978: A method for forecasting the arrival of cold surges in Hong Kong. Royal Observatory Hong Kong Tech. Note 43, 31 pp. [Available from the Royal Observatory Hong Kong, 134A Nathan Road, Hong Kong.]

Ding, Y., 1994: *Monsoons over China.* Kluwer Academic Publishers, 510 pp.

——, and T. N. Krishnamurti, 1987: Heat budget of Siberia high and the winter monsoon. *Mon. Wea. Rev.,* **115,** 2428–2448.

——, and M. Xiao, 1992: A case study of development and structure of a cold surge in east Asia. *Second Int. Conf. on East Asia and West Pacific Meteorology and Climate,* Hong Kong, Hong Kong Meteor. Soc., 311–328.

——, S. Wen, and Y. Li, 1991: A study of dynamic structures of the Siberia high in winter (in Chinese). *Acta Meteor. Sin.,* **49,** 428–439.

Holton, J. R., 1979: *An Introduction to Dynamic Meteorology.* 2d ed. Academic Press, 391 pp.

Palmen, E., and C. W. Newton, 1969: *Atmospheric Circulation Systems—Their Structure and Physical Interpretation.* International Geophysics Series, Vol. 13, Academic Press, 603 pp.

Qiu, Y. Y., 1988: A case study on the intense cold wave accompanied by the polar front over east Asia. *Extratropical Cyclones: The Erik Palmén Memorial Volume,* C. Newton and E. Holopainen, Eds., Amer. Meteor. Soc., 150–156.

Xie, A., Y. Lu, and S. Chen, 1992: The evolution of Siberia high to the outbreak of cold air (in Chinese). *Sci. Atmos. Sin.,* **16,** 677–685.

Wu, M. C., and J. C. L. Chan, 1995: Surface features of winter monsoon surges over South China. *Mon. Wea. Rev.,* **123,** 662–680.